ELSEVIER

Journal of Molecular Catalysis A: Chemical 144 (1999) 315–321

JOURNAL OF MOLECULAR CATALYSIS A: CHEMICAL

www.elsevier.com/locate/molcata

Electrocatalytic mechanism for formaldehyde oxidation on the highly dispersed gold microparticles and the surface characteristics of the electrode

Hui Yang [a], Tianhong Lu [a,*], Kuanhong Xue [b], Shigang Sun [c], Guoqiang Lu [c], Shenpei Chen [c]

[a] *Changchun Institute of Applied Chemistry, Chinese Academy of Sciences, Changchun 130022, China*
[b] *Department of Chemistry, Nanjing Normal University, Nanjing 210097, China*
[c] *Department of Chemistry, Xiamen University, Xiamen 361005, China*

Received 26 February 1998; accepted 13 October 1998

Abstract

Electrocatalytic mechanism for the electrochemical oxidation of formaldehyde (HCHO) on the highly dispersed Au microparticles electrodeposited on the surface of the glass carbon (GC) electrode in the alkaline $Na_2CO_3/NaHCO_3$ solution and the surface characteristics of the Au microparticle-modified glass carbon (Au/GC) electrode were studied with in situ FTIR spectroscopy, scanning electron microscopy (SEM) and X-ray diffraction (XRD). It was found that the final products of HCHO oxidation is $HCOO^-$ at the Au/GC electrode and CO_2 at the bulk Au electrode. The difference may be ascribed to the different surface characteristics between the Au/GC electrode and the bulk Au electrode.

Keywords: Formaldehyde; Gold microparticles; Electrochemical oxidation; FTIR

1. Introduction

The electrochemical oxidation of small organic molecules at precious metal (e.g., Pt, Pd, Au) electrodes has been extensively investigated. Among the precious metals, gold exhibits the good electrocatalytic activities in the electrochemical oxidation of HCHO [1–5] and CO [6,7] in alkaline media. The electrochemical oxidations of HCHO and CO are the interesting projects since HCHO and CO are the intermediates in the electrochemical oxidations of small organic molecules. Some investigators [1–3] proposed the electrochemical oxidation mechanisms of HCHO based on the possible species on the Au surface in the NaOH solutions. Avramov-Ivic et al. [4] have used the cyclic voltammetry combined with electrochemically modulated infra-red spectroscopy (EMIRS) to study the formation of the oxidation of the gem-diol form [$H_2C(OH)O^-$] of HCHO and formation of an adsorbed formate species during the oxidation of HCHO at the Au electrode in the 1 M NaOH solution.

* Corresponding author

1381-1169/99/$ - see front matter
PII: S1381-1169(98)00356-2

The preparation of the electrocatalysts with high performance is one of the most important subjects in electrolysis. An important method to obtain electrocatalysts with high performance and low cost is to disperse electrocatalytic materials onto the supporters, such as carbon or oxides [8]. In our previous paper [9], the electrochemical dispersion of Au microparticles onto the surface of the GC electrode and the electrocatalytic activities of the modified electrode for the oxidation of HCHO in the alkaline $Na_2CO_3/NaHCO_3$ solution were investigated. The results indicated that the Au microparticles with a few tens of nanometers in diameter can be uniformly distributed onto the surface of the GC electrode and the Au/GC electrode showed the electrocatalytic activity for the oxidation of HCHO higher than that of the bulk Au electrode. In this paper, an oxidation mechanism of HCHO at the Au/GC electrode in the alkaline $Na_2CO_3/NaHCO_3$ solution was proposed and compared with that at the bulk Au electrode. Then, it was explained why the Au/GC electrode showed the higher electrocatalytic activity for the oxidation of HCHO than the bulk Au electrode.

2. Experimental

Paraformaldehyde (Aldrich Chemicals) was refluxed for 4 h in order to obtain pure HCHO verified by FTIR spectroscopy. All other chemicals were of analytical grade. Solutions were prepared with triple distilled water. The solutions were deaerated by bubbling high-purity nitrogen before all measurements. The bubbling was continued during the in situ FTIR measurements.

Electrochemical and in situ FTIR measurements were performed using a potentiostat with a built-in waveform generator (Type XHD-I, Department of Chemistry and Factory of Fine Machinery, Xiamen University) and three-electrode electrochemical cell. The working electrode was the GC, Au or Au/GC electrode. The counter electrode was a platinized Pt electrode. A saturated calomel electrode (SCE) served as the reference electrode. All the potential were reported with respect to the SCE.

Before use, the GC (0.30 cm in diameter) or Au (0.38 cm in diameter) electrode was prepared as in the previous work [9]. Electrodispersion of Au microparticles onto the surface of the GC electrode was carried out in the 5 mM $HAuCl_4 + 0.5$ M HCl + 0.25 M H_2SO_4 solution with single potential step technique, typically from 0.80 to 0.43 V. The desired deposition amount of Au was controlled by the concurrent measurement of the charge passed at variable times. An aging treatment was applied to each electrode before measurements as in the previous work [9]. All the experiments were performed at the temperature of 25 ± 1°C.

The in situ FTIR spectroscopic experiments have been described in details elsewhere [10]. The difference spectra were obtained as $\Delta R/R = [R(E_2) - R(E_1)]/R(E_1)$, where $R(E_2)$ and $R(E_1)$ are the single beam spectra obtained at E_2 and E_1, respectively. In the difference spectra, the positive-going bands indicate that the IR adsorption at E_1 is greater than that at E_2 and the negative-going bands correspond to the greater IR absorption at E_2 than that at E_1. Usually, the number of interferograms (N.I.) collected at 8 cm^{-1} resolution was 20. When the intensities of the spectra are low, the large N.I. were used and noted in the figures. The surface distribution of Au microparticles electrodeposited onto the GC surface was examined with SEM (Model S-520, Hitachi, Japan). The XRD experiments were carried out on a Rigaku Rolaflex-C instrument with a rotating anode (Japan).

3. Results and discussion

According to the cyclic voltammetric results [9], HCHO is oxidized when the potential is higher than 0 V at the Au/GC electrodes. Fig. 1 presents a series of in situ FTIR spectra by

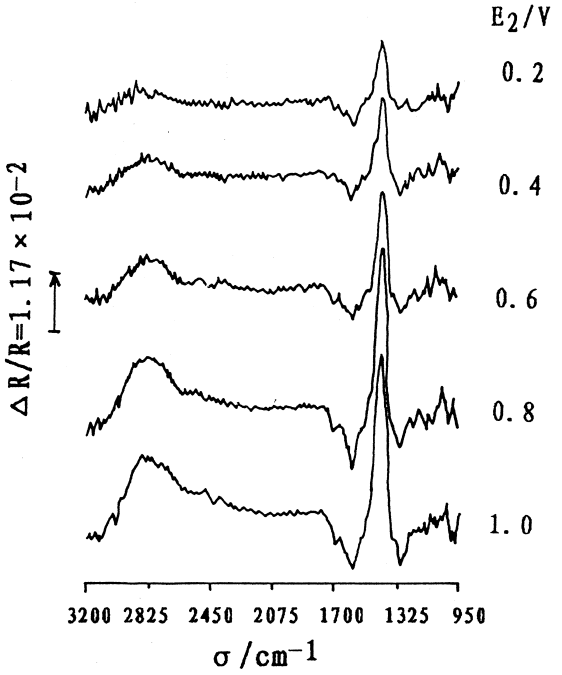

Fig. 1. In situ FTIR spectra at the Au/GC electrode in 0.1 M HCHO + 0.1 M Na_2CO_3 + 0.1 M $NaHCO_3$ at $E_1 = -0.8$ V and varying E_2.

fixing E_1 at -0.8 V and varying E_2 from 0.2 V to 1.0 V for the oxidation of HCHO in the 0.1 M HCHO + 0.1 M Na_2CO_3 + 0.1 M $NaHCO_3$ solution. The amount of the Au electrodeposited onto the surface of the GC electrode is ca. 19.6 $\mu g/cm^2$. Three positive-going bands can be observed from the spectra in Fig. 1 at about 2860, 1405 and 1050 cm^{-1}. They correspond to the stretch of C–H of HCHO molecule, the asymmetrical stretch of CO_3^{2-} and the IR absorption of the gem-diol form [$H_2C(OH)O^-$] of HCHO [11], respectively. Thus, they denote on the consumption of HCHO, the concentration decrease of CO_3^{2-} in the thin layer between the electrode and the IR window (CaF_2) and the consumption of [$H_2C(OH)O^-$], respectively, during the oxidation of HCHO at E_2. In addition, the increase in the intensities of the positive-going bands at 2860 and 1405 cm^{-1} with increasing E_2 indicated that the consumption amounts of HCHO and CO_3^{2-} increase with increasing E_2. There are also five negative-going bands in the spectra in Fig. 1. The negative-going bands at 1296 and 1677 cm^{-1} corresponding to the absorption of HCOOH molecule and at 1340 and 1587 cm^{-1}, corresponding to the absorption of $HCOO^-$ denote on the production of formic acid and formate. A negative-going band near 980 cm^{-1} corresponding to the weak absorption of HCO_3^- shows the concentration increase of HCO_3^- in the thin layer during the oxidation of HCHO at E_2. No absorption band near 2345 cm^{-1} corresponding to the asymmetrical stretch of CO_2 was observed during the oxidation process of HCHO.

Fig. 2 shows a series of in situ time resolved FTIR spectra by fixing E_1 at -0.8 V and E_2 at 0.5 V (Fig. 2A) and 1.0 V (Fig. 2B) at different times for HCHO oxidation at the Au/GC electrode in the 0.1 M HCHO + 0.1 M Na_2CO_3 + 0.1 M $NaHCO_3$ solution. It can be observed that the band positions in the spectra in Fig. 2 do not shift with, but the intensities of the bands change with the time. For example, the positive-going bands at 2860 and 1405 cm^{-1} firstly increase with the time and then remain unchanged, indicating the concentrations of HCHO and CO_3^{2-} decrease with the time and finally reach stable values at time > 3.96 s. It is interesting to note that the negative-going bands at 1296 and 1677 cm^{-1} corresponding to the product of HCOOH and at 1340 and 1587 cm^{-1} corresponding to the product of $HCOO^-$ appear from the beginning of the HCHO oxidation. Their intensities increase with time and then remain unchanged. These results definitely show that HCOOH and $HCOO^-$ do exist when HCHO is oxidized at the Au/GC electrode. From Figs. 1 and 2, it can be also seen that the band positions do not shift with the change of E_2 and with the time, suggesting that there are no adsorbed species on the surface of the Au/GC electrode during the oxidation of HCHO.

Considering the above results and that the gem-diol form [$H_2C(OH)O^-$] of HCHO [12] is the reactive species for the oxidation of HCHO at the Au electrode in an alkaline solution, the oxidation mechanism of HCHO in the weak

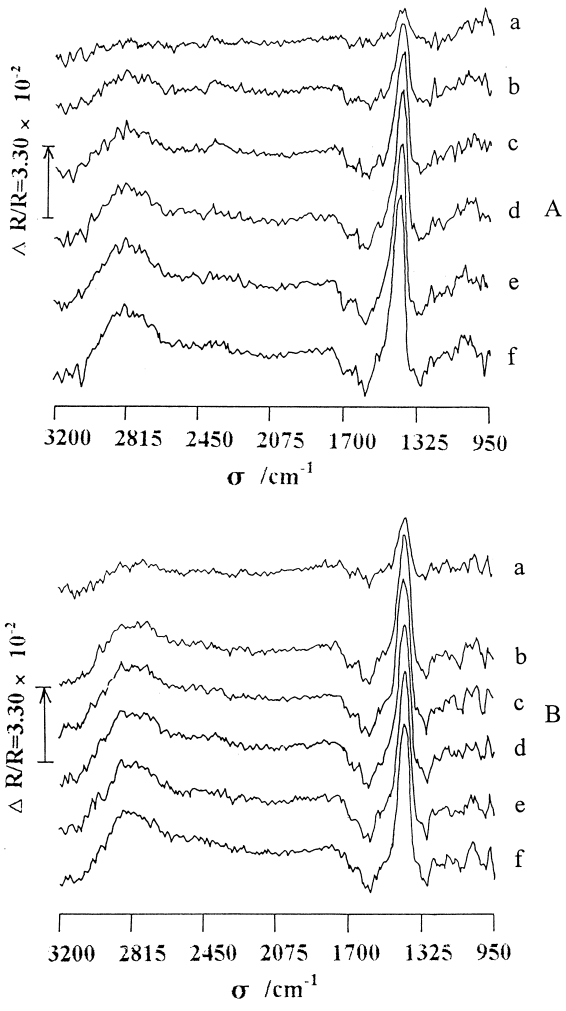

Fig. 2. In situ FTIR spectra at the Au/GC electrode in 0.1 M HCHO + 0.1 M Na_2CO_3 + 0.1 M $NaHCO_3$ at $E_1 = -0.8$ V and E_2 = (A) 0.5, (B) 1.0 V for the time (a) 0.44, (b) 1.32, (c) 2.20, (d) 3.08, (e) 3.96, (f) 4.84 s.

alkaline $Na_2CO_3/NaHCO_3$ system at the Au/GC electrode can be proposed as follows.

$$HCHO + OH^- = H_2C(OH)O^- \quad (1)$$

$$H_2C(OH)O^- = HCOOH + 1/2H_2 + e \quad (2)$$

$$HCOOH + OH^- = HCOO^- + H_2O \quad (3)$$

The overall reaction can be written as:

$$HCHO + 2OH^- = HCOO^- + H_2O + 1/2H_2 + e. \quad (4)$$

According to the above mechanism, the consumption of OH^- and the production of H_2O are obvious during the oxidation of HCHO. When one HCHO molecule is oxidized to $HCOO^-$, two OH^- anions are consumed and one H_2O molecule is produced. In turn, the consumption of OH^- anions and the production of H_2O molecules cause the right-shift of the following equation:

$$CO_3^{2-} + H_2O = HCO_3 + OH^- \quad (5)$$

It leads to the consumption of CO_3^{2-} and the production of HCO_3^- in the IR thin layer and the increase in the intensity of the positive-going CO_3^{2-} band with increasing E_2. Considering that the absorption bands of HCO_3^- and $[H_2C(OH)O^-]$ anions are located at 980 and 1028 cm^{-1}, where the CaF_2 window is opaque to IR with wave number less than 1000 cm^{-1}, it is impossible to evaluate the intensity changes of HCO_3^- and $[H_2C(OH)O^-]$ bands.

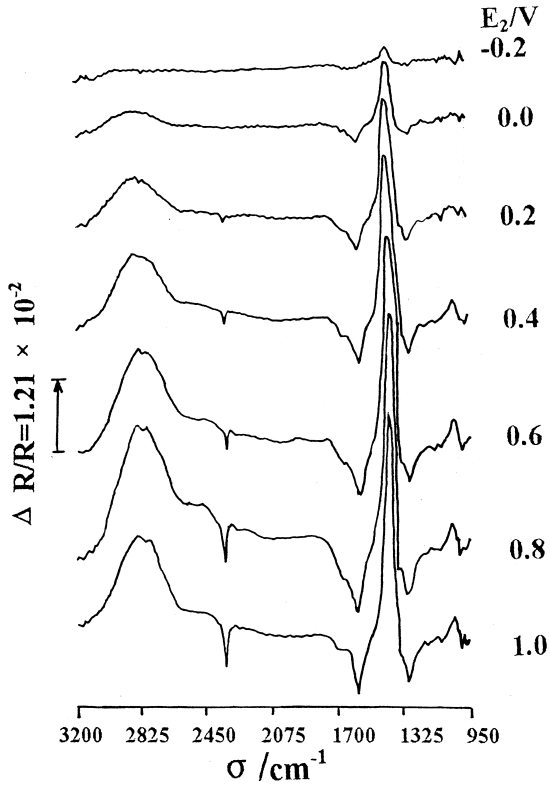

Fig. 3. In situ FTIR spectra at the bulk Au electrode in 0.1 M HCHO + 0.1 M Na_2CO_3 + 0.1 M $NaHCO_3$ at $E_1 = -0.8$ V and varying E_2.

Fig. 3 shows a series of in situ FTIR spectra of the HCHO oxidation by fixing E_1 at -0.8 V and varying E_2 from -0.2 to 1.0 V at the bulk Au electrode in the same solution. As can be seen, the spectra in Figs. 1 and 3 are similar except that the negative-going band near 2345 cm^{-1}, which corresponds to the asymmetrical stretch of CO_2, only appears in Fig. 3. It implies that the mechanism of HCHO oxidation at the Au/GC electrode differs from that at the bulk Au electrodes. The final product of HCHO oxidation at the Au/GC electrode is $HCOO^-$, while one of the products at the bulk Au electrode is CO_2 except the $HCOO^-$.

The cyclic voltammetric results showed that no oxidation peak was observed in the potential range between -0.40 and 1.0 V at different scan rates at the bare GC electrode in the 0.1 M HCHO + 0.1 M Na_2CO_3 + 0.1 M $NaHCO_3$ solution. A series of the in situ FTIR spectra (Fig. 4) for the HCHO oxidation recorded by fixing E_1 at -0.4 V and varying E_2 from 0 to 1.0 V at the bare GC electrode showed that the oxidation reaction of HCHO may take place when E_2 is more positive than 0.1 V. Comparing the N.I. and the $\Delta R/R$ values in Figs. 1 and 4, it can be found that the oxidation rate of HCHO at the bare GC electrode is much lower than that at the Au/GC electrode. However, the features of the spectra in Fig. 4 are similar to that at the Au/GC electrode in Fig. 1. The results imply that the oxidation of HCHO at the Au/GC electrode is affected by both Au microparticles and the GC substrate. The GC substrate restricts the product of the HCHO oxidation to be $HCOO^-$, while the Au microparticles greatly increase the electrocatalytic activity for the HCHO oxidation.

The electrodispersion of Au microparticles onto the surface of the GC electrode was carried out as in the previous work [9]. Fig. 5 presents the SEM micrographs of the Au/GC electrodes after electrochemical aging treatments. It can be seen from Fig. 5 that the Au microparticles are uniformly distributed on the surface of the GC electrode and the particle sizes are around 80–90 nm in diameter. Comparing (a) with (b) in Fig. 5, it can be seen that the particle distribution densities increase and the particle sizes have little change with increasing the deposition amount of Au microparticles.

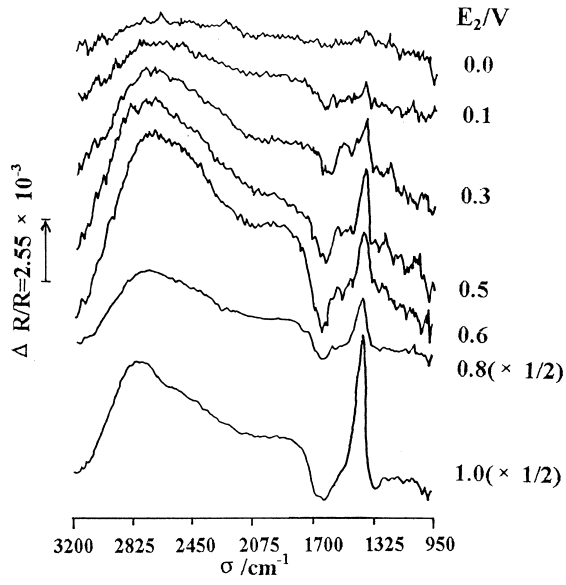

Fig. 4. In situ FTIR spectra at the bare GC electrode in 0.1 M HCHO + 0.1 M Na_2CO_3 + 0.1 M $NaHCO_3$ at $E_1 = -0.4$ V and varying E_2. N.I. = 400.

Fig. 6 shows the XRD spectra of the bare GC electrode (spectrum a) and the Au/GC electrode (spectrum b). In spectrum (a), 4 main diffractional peaks located at 43.1°, 53.0°, 78.8° and 93.2° were observed. They represent the XRD characteristics for the bare GC (similar to the diffractional peaks of graphite or diamond) [8]. When Au was electrodeposited onto the GC surface, except the peaks in spectrum (a), the XRD peaks corresponding to the different planes of the bulk Au crystallite were observed in spectrum b. However, because of the effect of the GC substrate, some crystal planes such as (400), (331), (420), (422) related to the bulk Au disappeared. The ratio of the intensity of the peak corresponding to (111) plane to those for (200), (220), (311) or (222) plane is higher than the data obtained from the Au powder diffraction (JCPDS Card No: 4-784), implying that the crystal of Au has a tendency to be preferentially

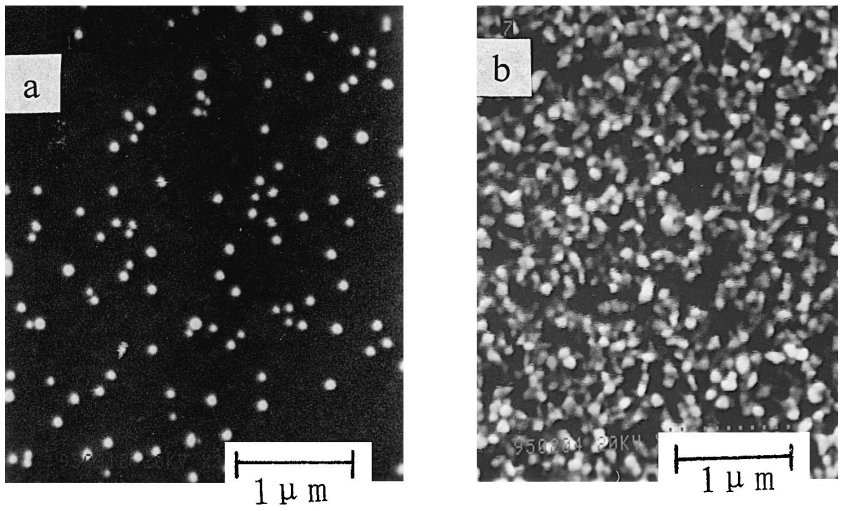

Fig. 5. The SEM micrographs of the Au/GC electrodes with (a) 4.9, (b) 22.0 μg/cm^2 Au microparticles after the electrochemical ageing treatment.

oriented due to the electrodeposition and the aging process. It may be ascribed to the phenomena of the poly-orientation of a single crystal and mono-orientation of polycrystalline in nature under certain conditions [13,14]. From the structural differences between the bulk Au and the Au on the GC surface, it can be inferred that the structural characteristics of the Au/GC electrode are favored to form $HCOO^-$ as the final product in the HCHO oxidation process, while the HCHO oxidation at the bulk Au electrode can form CO_2. Therefore, the fact that the oxidation of HCHO at the Au/GC electrode is faster than that at the bulk electrode [9] may be due to the fact that the product of HCHO oxidation at the Au/GC electrode is different from that at the bulk Au electrode.

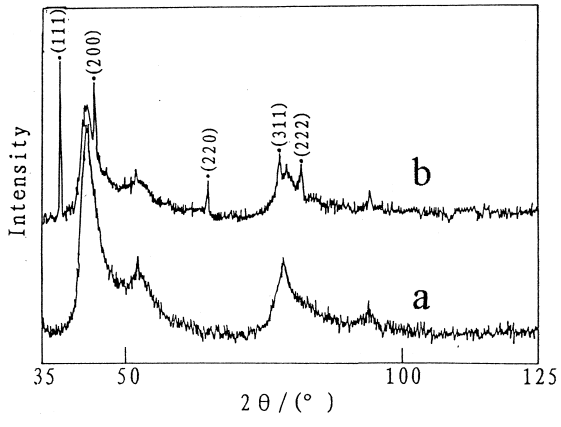

Fig. 6. The XRD spectra of (a) the bare GC electrode and (b) the Au/GC electrode with 22.0 μg/cm^2 Au microparticles.

In summary, in situ FTIR spectra demonstrated that in the alkaline $Na_2CO_3/NaHCO_3$ solution, the final product for the HCHO at the Au/GC electrode is $HCOO^-$ and the HCHO oxidation at the bulk Au electrode can form CO_2. It is the cause of why the HCHO oxidation at the Au/GC electrode is faster than that at the bulk Au electrode. Based on the SEM and XRD results, it can be suggested that the difference between the HCHO oxidation mechanisms at the Au/GC electrode and the bulk Au electrode is due to the effect of the GC substrate and the different surface characteristics, such as the different Au crystal orientations on the surfaces of the Au/GC and bulk Au electrodes.

Acknowledgements

This work is supported by the State Key Laboratory for Physical Chemistry of the Solid Surface, Xiamen University, P.R. China.

References

[1] B.B. Maria, Electrochim. Acta 30 (1992) 1193.
[2] L.D. Burke, J.J. O'Dwyer, Electrochim. Acta 35 (1990) 1829.
[3] L.D. Burke, W.A.O. Leary, J. Appl. Electrochem. 19 (1989) 758.
[4] M.L. Avramov-Ivic, R.R. Adzic, A. Bewick, J. Electroanal. Chem. 240 (1988) 161.
[5] M.L. Avramov-Ivic, N. Anastasijevic, R.R. Adzic, Electrochim. Acta 35 (1990) 161.
[6] H. Kita, H. Nakajima, J. Electroanal. Chem. 190 (1985) 140.
[7] L.D. Burke, V.J. Cunnane, J. Electroanal. Chem. 210 (1986) 69.
[8] S. Chen, S. Sun, T. Huang, Chin. Sci. Bull. 40 (1995) 377.
[9] H. Yang, T. Lu, K. Xue, S. Sun, S. Chen, J. Appl. Electrochem. 27 (1997) 428.
[10] S. Sun, D. Yang, Z. Tian, J. Electroanal. Chem. 289 (1990) 177.
[11] R.M. Silverstein, Spectrometric Identification of Organic Compounds, Wiley, New York, 1974.
[12] N. Tateishi, K. Nishimura, K. Yajikozawa, J. Electroanal. Chem. 352 (1993) 243.
[13] A.J. Aria, Electrochim. Acta 31 (1986) 1359.
[14] M.P. Sumino, S. Shibata, J. Electroanal. Chem. 322 (1992) 391.